Since benzhydrol absorbs light in the same wavelength region as the photocatalyst, special conditions were required to ensure exclusive excitation of the catalyst when this substrate was used. A dilute solution (6.5×10^{-4} M) of benzhydrol in a saturated solution of photocatalyst gave >99% light adsorption by the heteropolyoxotungstate. Similar concentration adjustments were also made with the benzylic substrates (Table VII). Products and relative rates of oxidation are listed in Tables VI and VIII.

Actinometry. Standard ferrioxalate actinometry methods were employed.[45] All manipulations were conducted in the dark or under a safety light. Pairs of light-opaque samples were irradiated in symmetrically placed vessels about the irradiation source for identical irradiation periods. Photocatalyst reduction was determined spectroscopically at 645 nm, and product yields were determined by GC or HPLC against an internal standard. An absolute measurement of the quantum efficiency of **1** was made, and all other measurements are reported relative to this absolute value.

Determination of the Extinction Coefficient of Reduced Heteropolytungstate. A dilute solution of **1** (2.0×10^{-4} M) or other heteropolytungstate was exhaustively irradiated under argon to a constant absorption at 690 nm. Identical absorption was attained by treatment under argon with excess zinc metal. Extinction coefficients were then calculated from the Beer-Lambert law.

Regeneration of the Photocatalyst. The exhaustively reduced solutions described above were opened to air and, while stirring, a UV-vis spectrum was recorded at 30-s intervals (Figure 1).

Electrochemistry. Cyclic voltammograms were recorded in a three-electrode cell[43] using a 1.2-mm platinum disk as the working electrode, a Pt foil flag or coil as the counter electrode, and a $Ag/AgNO_3$ reference. All compounds were analyzed as 1×10^{-3} M solutions with 0.1 M tetrabutylammonium perchlorate (TBAP) as electrolyte. Peak positions observed are listed in Table V.

Bulk electrolysis was carried out in a two-cell compartment similar to the analytical cell except that a mercury pool was employed as the working electrode. Under controlled potential, current flow was measured by digital coulometry.

NMR Complexation. A saturated solution of **1** in deuteriated acetonitrile was prepared. Two drops of alcohol were added and the spectrum was recorded. The comparison shown in Figure 4 was made with an identical concentration of alcohol in neat CD_3CN.

Acknowledgment. This work was supported by the Army Research Office. We happily acknowledge the technical assistance of Dr. Stephen Atherton of the Center for Fast Kinetics Research, a facility supported by the National Institutes of Health and by The University of Texas where the flash photolysis and single-photon-counting experiments were conducted. We are grateful to Professor Richard Finke, University of Oregon, for the samples of the vanadium-containing tungstates examined here and for extremely helpful discussions and suggestions.

(45) Hatchard, C. G.; Parker, C. A. *Proc. R. Soc. London, Ser. A* **1956**, *A235*, 518.
(46) Hardee, K. L.; Bard, A. J. *J. Electrochem. Soc.* **1977**, *124*, 215.

Complementarity and Chiral Recognition: Enantioselective Complexation of Bilirubin

David A. Lightner,* Jacek K. Gawroński, and W. M. Donald Wijekoon

Contribution from the Department of Chemistry, University of Nevada, Reno, Nevada 89557-0020. *Received April 27, 1987*

Abstract: Bichromophoric (4*Z*,15*Z*)-bilirubin-IXα, the cytotoxic pigment of jaundice, adopts either of two intramolecularly hydrogen-bonded enantiomeric conformations that are in dynamic equilibrium in solution. Added cinchona alkaloids, such as quinine, caused dichloromethane solutions of bilirubin to become intensely circular dichroic ($|\Delta\epsilon| \simeq 130$ L·mol^{-1}·cm^{-1}) in the region of the pigment's long-wavelength UV-visible absorption band (~450 nm). The optically active base acts as a chiral solvating agent to induce an asymmetric transformation of bilirubin, whose intense bisignate circular dichroism Cotton effect is characteristic of intramolecular exciton coupling.

(4*Z*,15*Z*)-Bilirubin-IXα (BR-IX), the yellow-orange, lipophilic, cytotoxic pigment of jaundice, is produced in abundant quantities in mammals by catabolism of heme and is transported as an association complex with albumin to the liver for glucoronidation and excretion.[1] The structure of the pigment has long been of interest owing to its importance in nature and its unusual solubility properties. Although the constitutional structural was proved over 40 years ago by classical methods,[2] its conformational structure was revealed only recently—by X-ray crystallography[3] and NMR spectroscopy.[4] Perhaps the most striking aspect of the three-dimensional structure of BR-IX is its ability and marked tendency to form extensive intramolecular hydrogen bonds, which link the polar carboxylic acid and lactam functionalities (Figure 1). This has important implications for biological function. It governs the shape and polarity of the molecule and explains the tremendous solubility differences between BR-IX and its constitutional isomers with propionic acid groups *not* located at C-8 and C-12. It also reveals the BR-IX structure as a potentially equilibrating pair of conformational enantiomers that interconvert by breaking and remaking all of its intramolecular hydrogen bonds. As such, BR-IX may be viewed as a racemic mixture (of A and B, Figure 1), whose crystals[3a] and solutions in isotropic solvents are optically inactive. However, in the presence of a chiral solvating agent, the bilirubin conformational enantiomers may act as chiral substrates (or templates) for molecular recognition.[5] For example, in the presence of cyclodextrins[6] or albumins,[7] BR-IX exhibits optical activity.[8]

(1) Lightner, D. A.; McDonagh, A. F. *Acc. Chem. Res.* **1984**, *17*, 417-424.
(2) (a) Fischer, H.; Plieninger, H.; Weisbarth, O. *Hoppe-Seyler's Z. Physiol. Chem.* **1941**, *268*, 197-226. (b) Fischer, H.; Plieninger, H. *Hoppe-Seyler's Z. Physiol. Chem.* **1942**, *274*, 231-260.
(3) (a) Bonnett, R.; Davies, J. E.; Hursthouse, M. B.; Sheldrick, G. M. *Proc. R. Soc. London, Ser. B.* **1978**, *202*, 249-268. (b) LeBas, G.; Allegret, A.; Mauguen, Y.; DeRango, C.; Bailly, M. *Acta Crystallogr., Sect. B.* **1980**, *B36* 3007-3011.
(4) For leading references, see: Kaplan, D.; Navon, G. *Isr. J. Chem.* **1983**, *23*, 177-186.
(5) For leading references, see: Rebek, J., Jr. *Science (Washington, D.C.)* **1987**, *235*, 1478-1484.
(6) Lightner, D. A.; Gawroński, J. K.; Gawrońska, K. *J. Am. Chem. Soc.* **1985**, *107*, 2456-2461.
(7) For leading references, see: Lightner, D. A.; Reisinger, M.; Landen, G. L. *J. Biol. Chem.* **1986**, *261*, 6034-6038.

0002-7863/87/1509-6354$01.50/0

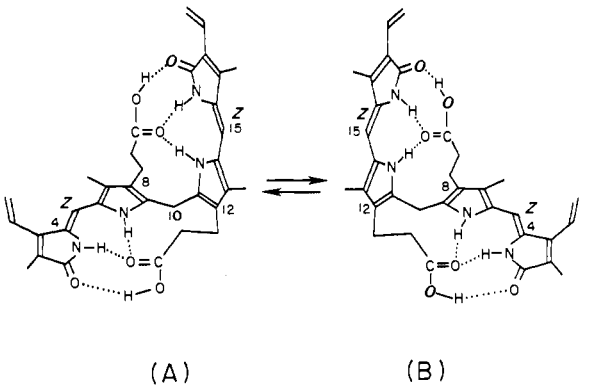

Figure 1. Interconverting, intramolecularly hydrogen-bonded enantiomeric conformers of bichromophoric (4*Z*,15*Z*)-bilirubin-IXα (BR-IX).

The origin of the optical activity may be understood as coming from nonequimolar concentrations of the *complexes* of enantiomers A and B (Figure 1). The position of the conformational equilibrium (A $\rightleftarrows$ B) of the uncomplexed mirror images A and B is expected to be unperturbed from $K_{eq} = 1$ to first approximation, neglecting anisotropic solvation effects. However, the same is not true for their complexes (S·A $\rightleftarrows$ S·B) with a chiral solute (S) because the complexes are diastereomeric, with different $\Delta G°_f$. Thus, the net concentration of A species [(A) + (S·A)] will not equal that of the B species [(B) + (S·B)], and the solutions will exhibit optical activity for the pigment. Optically active solutes that bind tightly to and are highly selective in forming heteroassociation complexes with one bilirubin enantiomer are expected to generate the most intense optical activity. This is seen with serum albumins, with which BR-IX exhibits circular dichroism (CD) Cotton effects (CEs) as high as $|\Delta\epsilon| \simeq 250$ L·mol^{-1}·cm^{-1} for porcine serum albumin[8b] but more typically in the range 20–50 L·mol^{-1}·cm^{-1}.[8] On the other hand, solutes that either do not have a large affinity constant or exhibit little selectivity for one enantiomer, e.g., cyclodextrins, generate weaker optical activity for BR-IX, with CD CEs in the range $|\Delta\epsilon| \simeq 5$–10 L·mol^{-1}·cm^{-1}.[6]

The factors that govern BR-IX binding to solutes like cyclodextrin and albumin are not well understood. However, a knowledge of the albumin binding capacity and the structure of its noncovalent bonded association complex with BR-IX have attracted considerable interest, for serum albumin serves not only as a vehicle for BR-IX transport but also as a biologic buffer against bilirubin encephalopathy or tissue damage in physiologic jaundice of the newborn.[9] The affinity of human serum albumin for BR-IX has been determined independently to be rapid, reversible, and strong, with an association constant of 10^7–10^8 for the first bilirubin and about an order of magnitude less for the second.[10] Although, the major ionic species between pH 6 and 9 is probably the monoanion,[11] it is conjectured that the bilirubin species that binds to albumin is the dianion (bispropionate anion),[12] with binding probably through amine (lysine) residues at the binding site on the protein.[13] With the possibility that chiral amines might be involved in the complexation of BR-IX on albumin and responsible for its intense optical activity, we initiated a program to explore the CD behavior of BR-IX with optically active amines.[14]

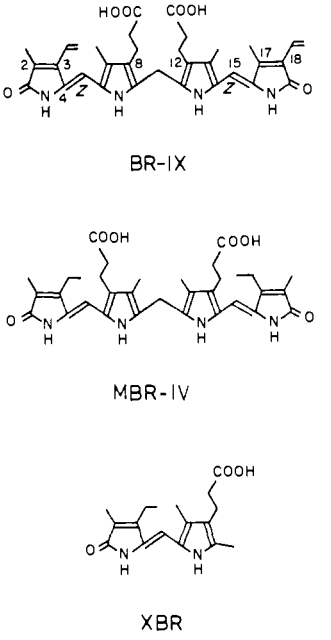

Figure 2. Linear structures of (4*Z*,15*Z*)-bilirubin-IXα (BR-IX), (4*Z*,15*Z*)-mesobilirubin-IVα (MBR-IV), and (4*Z*)-xanthobilirubic acid (XBR).

In the present work, we chose as optically active amines cinchona alkaloids, which are readily available, multifunctional amino alcohols capable of cooperative complexation[5] in catalytic action.[15] We will show that BR-IX can exhibit intense induced CD in the presence of these amines, whereas, its dimethyl ester shows only weak CEs. The studies are extended (1) to mesobilirubin-IVα (MBR-IV), a twin pyrromethenone bichromophoric analogue of BR-IX, but with both sets of propionic acid and methyl groups transposed on the central two pyrrole rings, and (2) xanthobilirubic acid (XBR), a monochromophoric analogue of BR-IX and MBR-IV. Analysis of the data provides an insight into potential mechanisms for the origin of the intense bisignate CDs observed with the albumin–BR-IX complex.

Experimental Methods

Quinine, quinidine, cinchonidine, cinchonine, and brucine were obtained from Aldrich. Bilirubin-IXα (BR-IX) contained <5% of the IIIα and XIIIα isomers as obtained from Sigma. Its dimethyl ester (BRDME) was isolated following reaction of BR-IX with CH_2N_2.[16a] Mesobilirubin-IVα (MBR-IV),[16b,c] its dimethyl ester (MBRDME),[16c] xanthobilirubic acid (XBR),[16e] and its methyl ester (XBRME)[16e] were prepared by total synthesis. The dichloromethane, methanol, and dimethyl sulfoxide solvents used were spectral grade. Pigment–amine solutions were prepared by dissolving the pigment in a freshly prepared alkaloid solution. All circular dichroism spectra were recorded within 15 min of solution preparation in a JASCO J-600 spectropolarimeter or on a JASCO J-40 spectropolarimeter equipped with a photoelastic modulator, and all UV–visible spectra were run on a Cary 219 spectrophotometer.

Results and Discussion

Molecular Structure and Induced Circular Dichroism. Bilirubin (Figure 1) owes its well-defined chiral secondary structure in the

(8) (a) For leading references, see: Blauer, G. *Isr. J. Chem.* **1983**, *23*, 201–209. (b) Harmatz, D.; Blauer, G. *Arch. Biochem. Biophys.* **1975**, *170*, 375–386. (c) Blauer, G.; Harmatz, D.; Snir, J. *Biochim. Biophys. Acta* **1972**, *278*, 68–88. (d) Blauer, G.; Harmatz, D. *Biochim. Biophys. Acta* **1972**, *278*, 89–100. (e) Blauer, G.; Lavie, E. In *Protein–Ligand Interactions*; Sund, H., Blauer, G., Eds.; W. de Gruyter: New York, 1975; pp 399–416.

(9) McDonagh, A. F.; Lightner, D. A. *Pediatrics* **1985**, *75*, 443–455.

(10) McDonagh, A. F. In *The Porphyrins*; Dolphin, D., Ed.; Academic Press: New York, 1979; Vol. 6, pp 293–491.

(11) Carey, M. C.; Spivak, W. In *Bile Pigments and Jaundice*; Ostrow, J. D., Ed.; Marcel Dekker: New York, 1986; pp 81–132.

(12) Brodersen, R. In *Bilirubin*; Heirwegh, K. P. M., Brown, S. B., Eds.; CRC Press: Boca Raton, FL, 1982; Vol. I, pp 75–123.

(13) Jacobsen, C. *Biochem. J.* **1978**, *171*, 453–459.

(14) That BR-IX can give induced CD in the presence of (+)- or (−)-α-phenylethylamine in organic solvents has been cited by Blauer in ref 8a and again in a discussion following a lecture by Blauer (ref 8e, p 409) for work of O. Mayer, Ph.D. Thesis, University of Konstanz, 1979. Our observations (J.-Y. An, unpublished data) with (*S*)-(−)-α-phenethylamine (Aldrich) in $CHCl_3$ solvent are $\Delta\epsilon^{414}_{max}$ +6.26 and $\Delta\epsilon^{472}_{max}$ −9.2 L·mol^{-1}·cm^{-1} for 4.5×10^{-5} M BR-IX, where the amine:BR-IX molar ratio is 15 000:1. In dimethyl sulfoxide, we could detect no CD.

(15) Wynberg, H. In *Stereochem.* **1986**, *16*, 87–129.

(16) (a) Lightner, D. A.; Trull, F. R. *Spectrosc. Lett.* **1983**, *16*, 785–803. (b) Trull, F. R.; Ma, J.-S.; Landen, G. L.; Lightner, D. A. *Isr. J. Chem.* **1983**, *23*, 211–218. (c) Trull, F. R.; Franklin, R. W.; Lightner, D. A. *J. Heterocycl. Chem.*, in press. (d) W. M. D. Wijekoon, this laboratory, from reaction of MBR-IV with CH_2N_2. (e) Lightner, D. A.; Ma, J.-S.; Franklin, R. W.; Landen, G. L. *J. Heterocycl. Chem.* **1983**, *21*, 139–144.

Table I. Circular Dichroism (CD) and Ultraviolet–Visible (UV) Spectral Data for 3.0×10^{-5} M Solutions of Bilirubin-IXα in Dichloromethane in the Presence of Alkaloid Bases at 21 °C[a]

alkaloid	alkaloid:bilirubin molar ratio	CD			UV	
		$\Delta\epsilon_1$ (λ_{max})	λ at $\Delta\epsilon = 0$	$\Delta\epsilon_2$ (λ_{max})	ϵ	λ_{max}
quinine	1:2	+0.5 (412)	433	−1.1 (464)		
	2:1	+1.8 (412)	433	−4.3 (465)	61 700	452
quinidine	1:2	−0.7 (415)	435	+1.4 (467)		
	2:1	−1.5 (415)	435	+3.0 (467)	61 200	452
cinchonidine	1:2	+0.6 (414)	438	−1.2 (468)		
	2:1	+1.5 (414)	438	−2.6 (468)	62 000	452
	1:2[b]	+1.0 (418)	438	−1.1 (470)		
	2:1[b]	+1.4 (418)	438	−2.5 (470)	61 200	454
	2:1[c]	+2.1 (418)	438	−3.7 (470)		
cinchonine	1:2	−1.8 (418)	440	+2.6 (468)		
	2:1	−2.2 (418)	440	+3.2 (468)	62 000	450
brucine	1:2	≪0.1 (462)		≪0.1 (413)		
	2:1	≪0.1 (462)		≪0.1 (413)	62 000	450

[a] Units: $\Delta\epsilon$, ϵ, L·mol^{-1}·cm^{-1}; λ, nm. These units are used in all subsequent tables. [b] Run in toluene at 21 °C. [c] Run in toluene at 0 °C.

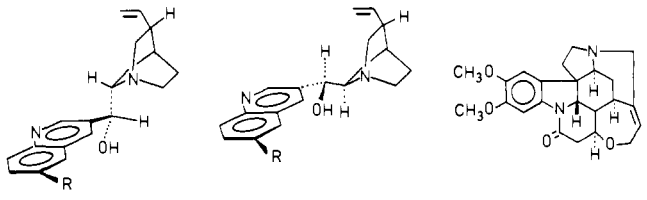

Figure 3. Structures and absolute configurations of cinchona alkaloids and brucine.

crystal and nonpolar solvents to (i) syn-periplanar conformations of the two pyrromethenone chromophores, each possessing *Z*-configuration carbon–carbon double bonds at C-4 and C-15, (ii) two propionic acid groups at C-8 and C-12, each capable of forming *intra*molecular hydrogen bonds with the opposing pyrromethenone lactam C=O/NH and pyrrole NH groups, and (iii) an sp^3 carbon at C-10, which keeps the two pyrromethenones 98–104° apart.[1,11] Even when BR-IX is deprotonated at the propionic acid groups, as in salts with amines[17] or tetraalkylammonium hydroxides,[18] the pigment retains a marked preference for the folded, intramolecularly H-bonded structures of the acid form. However, its dimethyl ester exhibits no unusual preference for this conformation,[11] tending instead to hydrogen bond *inter*molecularly in nonpolar solvents via a pyrromethenone-to-pyrromethenone dimeric arrangement akin to that observed with monochromophoric pigments such as XBR.[16a,b] Similarly, when the propionic acid groups are relocated away from C-8 and C-12, e.g., MBR-IV, the pigment is incapable of expressing intramolecular hydrogen bonding of the type shown (Figure 1). MBR-IV is therefore considerably more polar than BR-IX and is also readily excreted across the liver into bile without the necessity of glucuronidation.[19]

Bilirubin solutions in dichloromethane consist largely of equimolar concentrations of interconverting conformational enantiomers (A and B, Figure 1) and exhibit no optical activity.[1] However, addition of <1 molar equiv of a cinchona alkaloid produces a profound change: the solution exhibits CD (Table I) in the region of the pigment's long-wavelength UV–visible absorption band near 450 nm—a region where the alkaloid does not absorb light. In contrast, brucine, an alkaloid not *of* the cinchona family, shows no induced CD (ICD) at these (2:1) concentration ratios. Quinine and cinchonidine (Figure 3) induce nearly the same ICD behavior; their diastereomers, quinidine and cinchonine, respectively, induce oppositely signed CEs of nearly the same magnitudes. Except in the case of brucine, for which we can detect no ICD at either of these molar ratios, the CE magnitudes increase approximately twofold as the alkaloid:bilirubin molar ratio increases from 1:2 to 2:1. As shown in Tables II and III for quinine

Table II. Circular Dichroism (CD) Spectral Data for 3.0×10^{-5} M Solutions of Bilirubin-IXα in CH_2Cl_2, MeOH, and Me_2SO in the Presence of Quinine at 21 °C

quinine: bilirubin-IXα molar ratio	solvent	CD[a]		
		$\Delta\epsilon_1$ (λ_{max})	λ at $\Delta\epsilon = 0$	$\Delta\epsilon_2$ (λ_{max})
1:4	CH_2Cl_2	+0.3 (412)	432	−0.5 (462)
1:2	CH_2Cl_2	+0.5 (412)	433	−1.1 (464)
1:1	CH_2Cl_2	+1.0 (412)	433	−2.4 (465)
2:1	CH_2Cl_2	+1.8 (413)	433	−4.3 (465)
5:1	CH_2Cl_2	+5.5 (413)	433	−11.5 (465)
10:1	CH_2Cl_2	+10.0 (413)	434	−15.0 (465)
50:1	CH_2Cl_2	+41.0 (413)	434	−72.0 (465)
100:1	CH_2Cl_2	+50.5 (413)	434	−87.5 (465)
300:1	CH_2Cl_2	+74 (412)	433	−131 (465)
500:1	CH_2Cl_2	+75 (412)	433	−135 (465)
1000:1	CH_2Cl_2	+65 (411)	433	−120 (465)
10000:1[b]	CH_2Cl_2	+46 (405)	424	−100 (457)
100:1	MeOH	+3.3 (412)	433	−5.2 (465)
100:1	Me_2SO	*c*	*c*	*c*

[a] UV: $\epsilon_{max}^{452} = 61\,700 \pm 500$ (CH_2Cl_2) for all entries, except $\epsilon_{max}^{451} = 65\,000$ (MeOH); $\epsilon_{max}^{455} = 64\,000$ (Me_2SO). [b] CD bands begin to shift to shorter wavelengths due to overlap with strong CD bands from quinine. [c] No Cotton effects observed.

Table III. Circular Dichroism (CD) Spectral Data for 2.0×10^{-5} M Dichloromethane Solutions of Bilirubin-IXα in the Presence of Quinidine at 21 °C

quinidine: bilirubin-IXα molar ratio	CD[a]		
	$\Delta\epsilon_1$ (λ_{max})	λ at $\Delta\epsilon = 0$	$\Delta\epsilon_2$ (λ_{max})
1:4	−0.2 (415)	435	+0.5 (467)
1:2	−0.7 (415)	435	+1.4 (467)
1:1	−0.7 (415)	435	+1.6 (467)
2:1	−1.5 (415)	435	+3.0 (467)
10:1	−8.0 (415)	435	+13 (467)
100:1	−42 (415)	435	+70 (467)
1000:1	−65 (415)	435	+115 (467)

[a] UV: $\lambda_{max}^{452} = 61\,200 \pm 200$ (CH_2Cl_2) for all entries.

Table IV. Circular Dichroism (CD) Spectral Data for 2.0×10^{-5} M Dichloromethane Solutions of Bilirubin-IXα in the Presence of Brucine at 21 °C

brucine: bilirubin-IXα molar ratio	CD[a]		
	$\Delta\epsilon_1$ (λ_{max})	λ at $\Delta\epsilon = 0$	$\Delta\epsilon_2$ (λ_{max})
2:1	≪0.1 (462)		≪0.1 (413)
10:1	−0.8 (462)		≪0.1 (413)
100:1	−7.0 (462)	435	+5.0 (413)
1000:1	−14 (462)	435	+10 (413)

[a] UV: $\epsilon_{max}^{450} = 62\,000 \pm 1000$ (CH_2Cl_2) for all entries.

(17) Mugnoli, A.; Manitto, P.; Monti, D. *Acta Crystallogr., Sect. C* **1983**, *C39*, 1287–1291.
(18) Lightner, D. A.; Ma, J.-S.; Wu, X.-X. *Spectrosc. Lett* **1986**, *19*, 311–320.
(19) McDonagh, A. F.; Lightner, D. A., unpublished observations.

+ BR-IX and quinidine + BR-IX solutions, weak CEs can be detected even with alkaloid:BR-IX ratios as low as 1:4. The CEs in CH_2Cl_2 become extremely large with increasing ratios and then fall off somewhat at very high ratios. In contrast, brucine gives only relatively modest ICDs (Table IV), even for the high ratios. Whether the increasing $\Delta\epsilon$ magnitudes can be attributed simply to a mass law effect on an equilibrium producing a 1:1 cinchona alkaloid:pigment complex or whether they are due, e.g., to a 2:1 complex is presently unclear. However, since the $\Delta\epsilon$ values reach a plateau and then fall off with increasing alkaloid concentration (Table II), one is tempted to ascribe larger magnitude CEs to the 1:1 complex.

The CE magnitudes seen here with cinchona alkaloids approach the largest values ($\Delta\epsilon_{max}^{473}$ −214, $\Delta\epsilon_{max}^{423}$ +130 L·mol^{-1}·cm^{-1}) observed[8b] for BR-IX complexed to human serum albumin (HSA) [(BR-IX):(HSA) = 15, 0.83 × 10^{-5} M BR-IX, pH 4.05] and exceed those recorded[7] for HSA·BR-IX solutions near physiologic pH [$\Delta\epsilon_{max}^{460}$ +49, $\Delta\epsilon_{max}^{407}$ −26 L·mol^{-1}·cm^{-1}, pH 7.3, (HSA):(BR-IX) = 2], where it is the BR-IX dianion that is said to bind to HSA.[12] They contrast markedly with the considerably weaker CE magnitudes ($\Delta\epsilon_{max}^{460}$ −3.0, $\Delta\epsilon_{max}^{409}$ +2.4 L·mol^{-1}·cm^{-1}) for pH 8.0 BR-IX solutions with a 1000-fold molar excess of α-cyclodextrin,[6] and they greatly exceed the CE magnitudes of the only published CD spectra of BR-IX with chiral amines: ($\Delta\epsilon_{max}^{462}$ −7.8, $\Delta\epsilon_{max}^{407}$ +6.0 L·mol^{-1}·cm^{-1}) for a 100:1 molar ratio of *N*-acetyl-L-lysine-*N'*-methylamide:BR-IX in CH_2Cl_2 and ($\Delta\epsilon_{max}^{462}$ −9.9, $\Delta\epsilon_{max}^{420}$ +5.8, $\Delta\epsilon_{max}^{502}$ +7.1 L·mol^{-1}·cm^{-1}) for a 1:1 molar ratio of poly(L-lysine):BR-IX in H_2O at pH 11.4.[20]

The remarkably intense ICD CEs with cinchona alkaloids thus appear to be unprecedented for BR-IX in the presence of a simple optically active molecule. They suggest a high degree of enantioselectivity by a chiral solvating agent[21] for one of the bilirubin conformational enantiomers and a fairly strong coordination to it. High selectivity and strong binding, which are characteristic of protein–bilirubin complexation,[8a] appear to be mimicked here by cinchona alkaloids but not necessarily by other β-arylethylamines, e.g., brucine (Table IV). We assume that the complexation involves an acid–base equilibrium of the type shown in eq 1 and 2, where A and B are the BR-IX conformational enan-

$$A + S \overset{K_{eq}^1}{\rightleftharpoons} S{\cdot}A \quad (1)$$

$$B + S \overset{K_{eq}^2}{\rightleftharpoons} S{\cdot}B \quad (2)$$

tiomers (Figure 1), the chiral solvating agent, S, is an alkaloid (Figure 3), and $K_{eq}^1 \neq K_{eq}^2$. We take S·A and S·B to be diastereomeric amine salt complexes that are enantiomeric in BR-IX monoanions as illustrated in Figure 4, although the dianion complexes would serve equally well in the arguments that follow. The complexation process, however, with its apparently high enantioselectivity, would appear to involve more than merely an acid–base equilibrium. It seems likely that other aspects of molecular structure must play an important role in binding, including stereochemistry and complementarity in the binding process. In acting as a chiral template, the strong preferential selectivity of quinine for A and not B, or vice versa, probably involves a unique dissymmetric arrangement (asymmetric microenvironment)[5] of "multiple-point" binding features, including hydrogen bonding from the secondary hydroxyl group and van der Waals attractions between the alkaloid aromatic quinoline nucleus and the pigment's pyrromethenone moiety, in addition to the amine salt ionic bonding. The concept of multiple-point binding has been invoked recently by Rebek[5] in his models for molecular recognition and was advanced by Pirkle[21a] for chiral solvating agents in NMR studies[21b] and in resolutions by chromatographic methods. It is tempting therefore to predict the

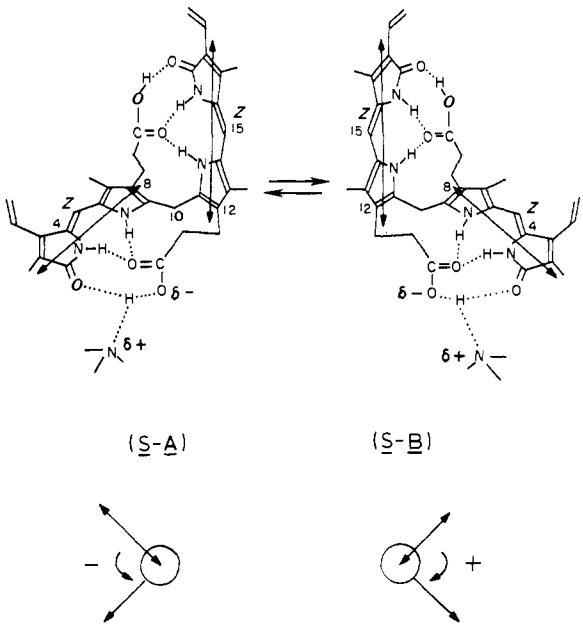

Figure 4. (Upper) Interconverting, intramolecularly hydrogen-bonded diastereomeric conformers of bichromophoric BR-IX salt complexes with chiral amines (*S*) such as the cinchona alkaloids of Figure 3. (Only the monosalts are shown for simplicity of representation.) The monoanion components of the complexes are enantiomeric in pigment conformation. The approximate directions[30] of the pyrromethenone chromophore electric transition dipole moments are given by the double-headed arrow. (Lower) The relative orientations of the electric dipole transition moments (viewed at C-10) of the pyrromethenone chromophores of S·A (left) and S·B (right). The S·A diastereomeric complex has left-handed (−) chirality of the two pyrromethenone chromophores; the S·B diastereomeric salt has right-handed (+) chirality.

feasibility of an optical resolution of (racemic) BR-IX by chromatography on adsorbents covalently bound to or polymers containing cinchona alkaloids.

The reaction of *dl*-bilirubin (A and B, Figure 1) with, e.g., quinine can be viewed as an example of a first-order asymmetric transformation,[22] where one salt is greatly favored over the other in the equilibrium

$$\text{quinine}{\cdot}d\text{-BR-IX complex} \rightleftarrows \text{quinine}{\cdot}l\text{-BR-IX complex} \quad (3)$$

but where the acidic component of the salt is labile and mutarotates. Indeed, attempts to liberate optically active BR-IX from its salt complex with quinine at −20 °C by washing the 100:1 and 1000:1 molar ratio (quinine:pigment) solutions in dichloromethane (Table II) with 2 N HCl gave recovered pigment with no CD detected at 465 nm. In preliminary experiments, we could not induce the quinine·BR-IX salts to crystallize at −25 °C.

In the equilibria depicted by eqs 1–3, a lowered solution temperature should produce more of the more stable complex, with a resultant increase in CD. This is observed for the 2:1 cinchonidine:BR-IX complex in toluene (Table I), where the magnitudes of the CEs seen at 21 °C double upon lowering to 0 °C. The equilibria can also be influenced by choice of solvent. Nonpolar solvents should support the tight ion-pair structures shown; polar hydrogen-bonding solvents should facilitate dissociation, either as a dissociated ion pair or, more likely, as separated acid base species: A or B and S. Thus, in solvents such as methanol or dimethyl sulfoxide, the CD CEs are expected (and found (Table II)) to be much weaker than in dichloromethane because less of the complex, S·A or S·B, is present.

The heteroassociation complexation (eq 1 and 2) apparently requires acid functional groups on the pigment and is not due uniquely to other forces, e.g., micellar, electrostatic, or π–π interactions, because the dimethyl esters of BR-IX and MBR-IV give only relatively weak CD CEs with quinine (Table V).[23] It

(20) Marr-Leisy, D.; Lahiri, K.; Balaram, P. *Int. J. Peptide Protein Res.* **1985**, *25*, 290–296. See also: Woolley, P. V., III; Hunter, M. J.; Arias, I. M. *Biochim. Biophys. Acta* **1976**, *446*, 115–123.

(21) (a) Pirkle, W. H.; Hoover, D. J. In *Top. Stereochem.* **1982**, *13*, 263–331. (b) Weisman, G. R. In *Asymmetric Synthesis*; Morrison, J. D., Ed.; Academic Press: New York, 1983; Vol. 1, pp 153–171.

(22) Turner, E. E.; Harris, M. M. *Q. Rev., Chem. Soc.* **1947**, 299–330.

Table V. Circular Dichroism (CD) and Ultraviolet–Visible (UV) Spectral Data for (1.0–3.0) × 10^{-5} M Solutions of Bilirubins in Dichloromethane in the Presence of Quinine at 21 °C

pigment	quinine:pigment molar ratio	CD			UV	
		$\Delta\epsilon_1$ (λ_{max})	λ at $\Delta\epsilon = 0$	$\Delta\epsilon_2$ (λ_{max})	ϵ	λ_{max}
bilirubin-IXα	300:1	+74 (412)	433	−131 (465)	61 000	452
bilirubin-IXα dimethyl ester	300:1	−3.3 (415)	442	+1.7 (470)	62 000	398
					27 000	450 (sh)
mesobilirubin-IVα	300:1	−6.5 (380)	402	+8.3 (438)	37 300	392
					15 000	430 (sh)
mesobilirubin-IVα dimethyl ester	300:1	−0.77 (386)	416	+0.62 (442)	30 300	378
					10 600	430 (sh)
xanthobilirubic acid	300:1	−5.0 (412)			30 500	410
xanthobilirubic acid methyl ester	300:1	−0.42 (410)			33 000	402

also requires pigments that can adopt and retain enantiomeric conformations such as A and B because MBR-IV, which is a diacid *in*capable of adopting the intramolecularly H-bonded conformations of Figures 1 and 4, shows only relatively weak CD CEs. Although MBR-IV is capable of forming amine salts, such diastereomeric complexes can assume a multitude of conformations, apparently with no strong preference for the unique, chiral conformations expressed by BR-IX (Figure 4). The induced CDs of the diesters BRDME and MBRDME, and possibly even MBR-IV, probably have their origin in general asymmetric solvation effects involving the alkaloid, possibly as a chiral template, and possibly of a nature similar to that which produces bisignate CD CEs for BRDME in ethyl (*S*)-(−)-lactate ($\Delta\epsilon^{410}_{max}$ −3, $\Delta\epsilon^{430}_{max}$ +2.5 L·mol^{-1}·cm^{-1}) and (*R*,*R*)-(−)-2,3-butanediol ($\Delta\epsilon^{405}_{max}$ −0.4, $\Delta\epsilon^{430}_{max}$ +0.8 L·mol^{-1}·cm^{-1}).[24]

Origin of Bisignate ICD Cotton Effects and Exciton Coupling. Bisignate CEs are characteristic of the ICD spectra of various bichromophoric molecules studied here: BR-IX, BRDME, MBR-IV, and MBRDME. The bisignate nature of the induced CD, with two oppositely signed CEs straddling the UV–visible transition(s), is typical of excited-state interaction in weakly coupled electronic systems (molecular exciton[25]).[26] Here, two pyrromethenone chromophores with strongly allowed long-wavelength electronic transitions ($\epsilon_{max} \simeq 30\,000$ L·mol^{-1}·cm^{-1}) have only a small interchromophoric electron overlap but interact through their locally excited states by resonance splitting (electrostatic interaction of the local transition moment dipoles). The exciton splitting gives rise to two long-wavelength UV–visible transitions, one higher in energy and one lower in energy, with the separation dependent on the strength and relative orientation of the (pyrromethenone) chromophore's electric dipole transition moments.[26,27] As seen in their UV–visible spectra, the two electronic transitions overlap to give the characteristically broadened absorption bands of bilirubinoids.[28] As seen in their CD spectra, the two exciton transitions are always oppositely signed, however, as predicted by theory,[26,27] and thus give rise to bisignate CEs. In contrast to UV–visible absorption curves, which may show only slight broadening when the exciton splitting energy is small, when two oppositely signed curves overlap in the CD, there is considerable cancellation in the region between the band centers with the net result that the *observed* bisignate CE maxima are displaced from the actual locations of the (uncombined) CD

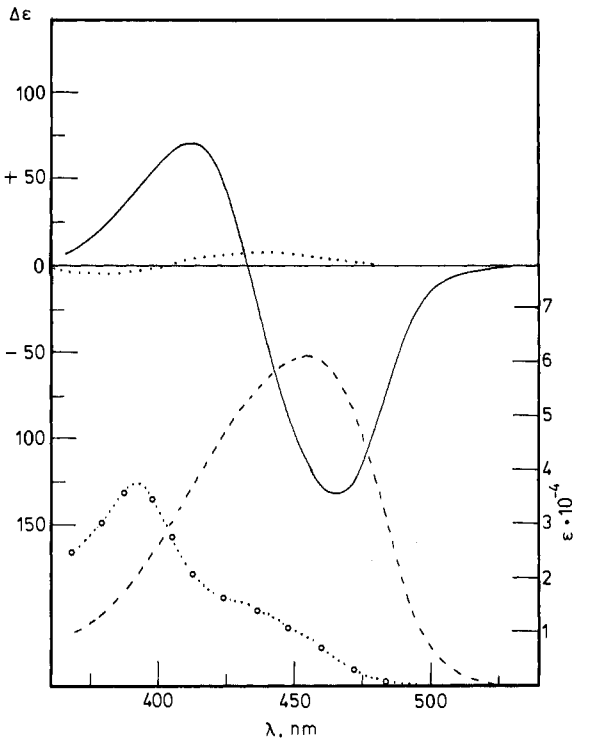

Figure 5. Circular dichroism (—) and UV–visible (---) spectra of 3.0 × 10^{-5} M bilirubin-IXα in dichloromethane in the presence of 9.0 × 10^{-3} M quinine at 21 °C. CD (···) and UV–visible (○) spectra of 3.0 × 10^{-5} M MBR-IV in dichloromethane in the presence of 9.0 × 10^{-3} M quinine at 21 °C. The spectra were recorded within 15 min after preparation of the solution and remained essentially invariant for 24 h at 22 °C. A CD spectrum of the same concentration of BR-IX without added quinine falls on the $\Delta\epsilon = 0$ line.

transitions[29] and typically are seen to flank the corresponding UV–visible band(s). This is amply illustrated with the ICD and UV–visible spectra of BR-IX in the presence of quinine (Figure 5) and may still be recognized in the much weaker bisignate ICDs of its dimethyl ester (Figure 5) or mesobilirubin-IVα and its dimethyl ester (Figure 6).

Bisignate CDs might also arise in bichromophoric bilirubins if each pyrromethenone acted independently to produce CEs of opposite signs. The optical activity might arise from asymmetric perturbation or induced dissymmetry of the chromophore—through the action of chiral solvation or ligating agents. However, we tend to believe that this mechanism is unimportant for explaining the large ICD CEs of BR-IX for the following reasons. (1) The monochromophoric molecular analogue, XBR, shows only weak monosignate CEs with added quinine (Table V and Figure 7), whereas the bichromophoric "acidic" pigments BR-IX and MBR-IV show bisignate ICDs. The origin of the monosignate

(23) These solutions, on standing for hours to days, show somewhat increased $\Delta\epsilon$ magnitudes, however, which we assume arise from transesterification to give pigment (mono)esters with the alkaloid.

(24) (a) Braslavsky, S. E.; Holzwarth, A. R.; Schaffner, K. *Angew. Chem., Int. Ed. Engl.* **1983**, *22*, 656–674. (b) Holzwarth, A. R.; Langer, E.; Lehner, H.; Schaffner, K. *J. Mol. Struct.* **1980**, *60*, 367–371. (c) Holzwarth, A. R.; Langer, E.; Lehner, H.; Schaffner, K. *Photochem. Photobiol.* **1980**, *32*, 17–26.

(25) Kasha, M.; Rawls, H. R.; El-Bayoumi, M. A. *Pure Appl. Chem.* **1965**, *32*, 371–392.

(26) For leading references and examples, see: Harada, N.; Nakanishi, K. *Circular Dichroic Spectroscopy—Exciton Coupling in Organic Stereochemistry*; University Science Books: Mill Valley, CA, 1983.

(27) Hug, W.; Wagnière, G. *Tetrahedron* **1972**, *28*, 1241–1248.

(28) The transition dipole probabilities of the two exciton transitions are not necessarily equal and will depend on the relative orientations of the electric dipole transition moments. Consequently, the shapes and positions of the long-wavelength absorption bands may be expected to vary with pigment conformation; cf. BR-IX vs BRDME and the latter in different solvents.

(29) This phenomenon has been discussed in detail previously and is shown graphically in Figures 1–4 of ref 26. See also: Wellman, K. M.; Lauer, P. H. A.; Briggs, W. S.; Moscowitz, A.; Djerassi, C. *J. Am. Chem. Soc.* **1965**, *87*, 66–72.

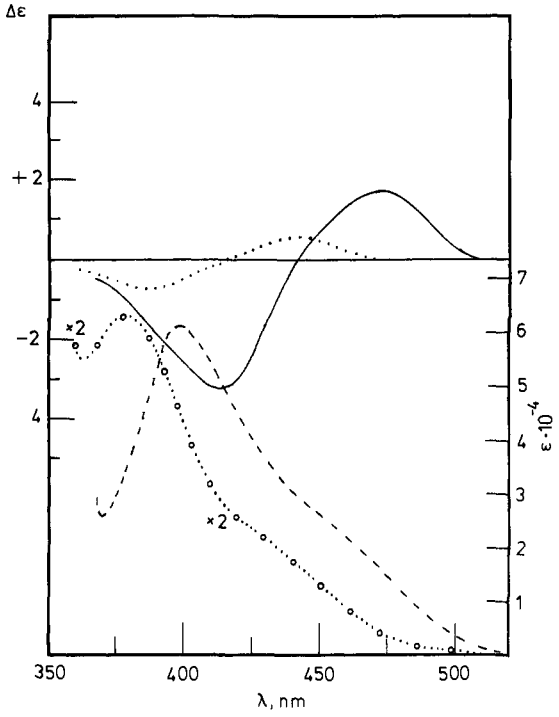

Figure 6. Circular dichroism (—) and UV-visible (---) spectra of 3.0 × 10^{-5} M bilirubin-IXα dimethyl ester in dichloromethane in the presence of 9.0 × 10^{-3} M quinine at 21 °C. CD (···) and UV-visible (○) spectra of 3.0 × 10^{-5} M mesobilirubin-IVα dimethyl ester in dichloromethane in the presence of 9.0 × 10^{-3} M quinine at 21 °C. The spectra were recorded within 15 min after preparation of the solution and remained essentially invariant for hours at 22 °C. (The UV curve for MBR-IV DME is scaled ×2 in Δε values.) A CD spectrum of the same concentration of BRDME or MBR-IV DME without added quinine falls on the Δε = 0 line.

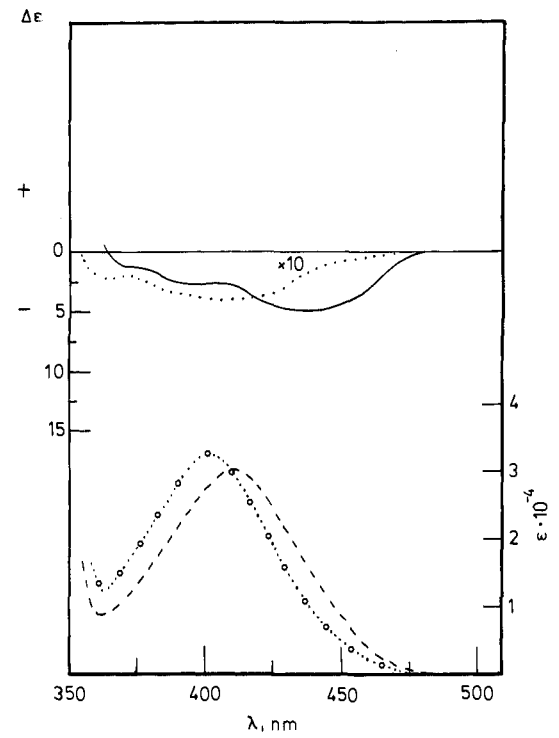

Figure 7. Circular dichroism (—) and UV-visible (---) spectra of 3.0 × 10^{-5} M xanthobilirubic acid in dichloromethane in the presence of 9.0 × 10^{-3} quinine at 21 °C. CD (···) and UV-visible spectra (○) of 3.0 × 10^{-5} M xanthobilirubic acid methyl ester in dichloromethane in the presence of 9.0 × 10^{-3} M quinine at 21 °C. The spectra were recorded within 15 min after preparation of the solution and remained essentially invariant for hours at 22 °C. (The CD curve of XBRME is scaled ×10 in Δε values for clarity of presentation.) A CD spectrum of the same concentration of XBRME without added quinine falls on the Δε = 0 line.

CE from XBR with quinine may come from an acid–base salt complex or from π–π London force[25] heteroassociation. (2) XBRME similarly gives only a monosignate ICD, in marked contrast to weak bisignate ICDs of BRDME and MBRDME. The origin of the weak monosignate CEs with XBRME + quinine probably comes from weak heteroassociation complexation of monomeric pigment to the quinine, possibly through the action of H-bonding or London forces.[25] (3) The CD couplets for the bichromophoric molecules are always of opposite sign—as required by the exciton model. If the chromophores were acting independently, one should expect to find both monosignate and bisignate ICDs for, e.g., BR-IX. However, this has not been observed.

Computed Absolute Configuration of Bilirubin–Quinine Complex. Exciton coupling theory[26] provides a way to assign the absolute configuration, either S·A or S·B (Figure 4), of the predominant complex. The CD (and UV) spectra of bilirubins can be calculated by treating the molecule as two isolated pyrromethenone chromophores (*i* and *j*) connected by single bonds but with no interchromophoric π-orbital overlap. Since electronic excitation (from the ground state $|0\rangle$ to the excited state $|q\rangle$, Figure 8) in either pyrromethenone involves a displacement of electronic charge from the chromophore's ground state to its excited state (charge density polarization), an electric transition dipole moment ($\vec{\mu}_{0q} = \langle 0|\nabla|q\rangle$ is created for each chromophoric excitation. The two transition dipole moments ($\vec{\mu}_{i0q}$ from pyrromethenone *i* and $\vec{\mu}_{j0q}$ from pyrromethenone *j*)[30] interact, and the excited states are said to couple or mix. This coupling of the strongly allowed, long-wavelength excited state of pyrromethenone *i* with the comparable excited state of pyrromethenone *j* gives a molecular excited state (exciton), which may be viewed as being delocalized between the two chromophores and is split in energy by dipole–dipole interaction (Figure 8).

If the pyrromethenone chromophores preserve their individuality in bilirubin, e.g., little or no electron overlap, application of perturbation theory[25,26] will give *molecular* electronic wave functions and energies in terms of the wave functions and energies of the pyrromethenone units. Since the ground-state energy level of each pyrromethenone is taken to be zero and the van der Waals interaction between the permanent dipoles is assumed to be very small,[25] the bilirubin molecular ground state is unsplit and also taken to be zero (Figure 8). In contrast, perturbation theory predicts both a nonzero resonance (Davydov) splitting and the splitting energy ($2\Delta E_{ij}$) of the bilirubin molecular excited state due to exchange of excitation energy between the two pyrromethenone chromophores (exciton coupling). The center of the splitting will be displaced downward from energy level *q* (E_q, Figure 8) by the dipole–dipole interaction energy between the permanent dipole of one pyrromethenone chromophore in its excited state and the other in its ground state.[25] This displacement is taken to be negligible here. Consequently, assuming for simplicity that the two pyrromethenone chromophores are identical, the energies of the two different molecular excited states, α and β, arising from exciton splitting will be given by

$$E^{\alpha} = E_{0q} - \Delta E_{ij} \quad (4)$$

$$E^{\beta} = E_{0q} + \Delta E_{ij} \quad (5)$$

where E_{0q} is the excitation energy ($0 \rightarrow q$) of the pyrromethenone chromophore, ΔE_{ij} is the dipole–dipole interaction energy between the two transition dipole moments of pyrromethenones, and $2\Delta E_{ij}$ is the exciton (Davydov) splitting energy. E_{0q} may be determined

(30) The direction of the electric dipole transition moment in the pyrromethenone chromophore has been calcualted by a π-electron SCF–MO–CI procedure (PPP approximation) to lie along the longitudinal axis of the planar conjugated π-system. Blauer, G.; Wagnière, G. *J. Am. Chem. Soc.* **1975**, *97*, 1949–1954. See also Falk et al. (Falk, H.; Grubmayr, K.; Höllbacher, G.; Hofer, O.; Leodolter, A.; Neufingerl, F.; Ribō, J. M. *Monatsh. Chem.* **1977**, *108*, 1113–1129) for the direction of the pyrromethenone transition dipole from linear dichroism measurements in cholesteric mesophases.

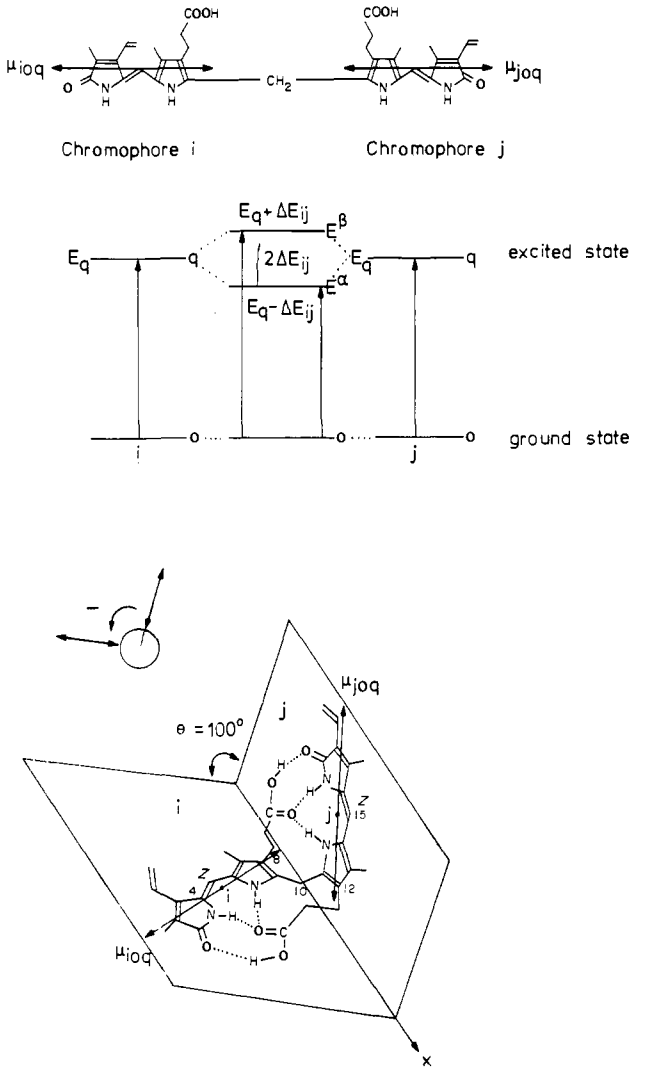

Figure 8. (Upper) The two pyrromethenone chromophores (*i* and *j*) of bilirubin-IXα. (Middle) State energy levels (0 = ground state, q = excited state) for pyrromethenone chromophores and their exciton interaction to give the bilirubin molecular electronic excited state with a Davydov splitting energy equal to $2\Delta E_{ij}$. For simplicity of representation, the two pyrromethenones (*i* and *j*) are taken to be identical. (Bottom) Left-handed (negative chirality) enantiomeric conformation of bilirubin used for exciton splitting calculation. Pyrromethenone units *i* and *j* lie in planes that intersect along the x axis. The z axis bisects the interplanar (dihedral) angle, θ, and intersects the x axis at C-10. The approximate locations of the electric dipole transition moments ($\vec{\mu}_{i0q}$ and $\vec{\mu}_{j0q}$) are drawn through the chromophores as double-headed arrows, and their helicity is indicated in the Newman-type drawing.

experimentally from the UV-visible spectrum or computed by MO methods,[30] and ΔE_{ij} may be calculated in the point dipole–point dipole approximation from the equation

$$\Delta E_{ij} = [\vec{\mu}_{i0q}\cdot\vec{\mu}_{j0q} - 3R_{ij}(\vec{\mu}_{i0q}\cdot\vec{R}_{ij})(\vec{\mu}_{j0q}\cdot\vec{R}_{ij})]R_{ij}^{-3} \qquad (6)$$

where $\vec{\mu}_{i0q}$ and $\vec{\mu}_{j0q}$ are the electric dipole transition moments of pyrromethenone chromophores *i* and *j*, respectively, and R_{ij} is the interchromophoric distance vector connecting the two transition moments. Since the pyrromethenone transition dipole moments $\vec{\mu}_{i0q}$ and $\vec{\mu}_{j0q}$ arise from charge density polarization by the long-wavelength excitation ($0 \rightarrow q$) and are thus proportional to the intensity of the electronic transition, the exciton splitting, $2\Delta E_{ij}$, will be large for this strongly allowed (π–π^*?) transition. The magnitude of the splitting also depends on the relative orientation of the pyrromethenone transition dipole moments and falls off as the inverse cube of the intermolecular distance, R_{ij}. For bilirubins, $2\Delta E_{ij}$ is smallest when the pyrromethenone chromophores are coplanar (180° interplanar angle).

In order to compute ΔE_{ij}, we make the simplifying assumption that the two pyrromethenone chromophores are identical and the same as that of the XBR chromophore; therefore, $\mu_{i0q} = \mu_{j0q}$. In the folded conformations of Figure 1 the angle (θ) between the two dipole moments is taken to be 100° since X-ray crystallographic studies[3,17] whow that the two pyrromethenones of bilirubin and mesobilirubin are essentially planar and their interplanar (dihedral) angle (θ) is 98–104°.[11] With the direction of polarization of μ_{i0q} and μ_{j0q} lying in the plane of the chromophore, approximately along the line connecting C-2 and C-8, $R_{ij} \simeq 6$ Å and $\vec{R}_{ij}$ makes angles of $\phi \simeq 50°$ with $\vec{\mu}_{i0q}$ and $\phi \simeq 130°$ with $\vec{\mu}_{j0q}$. Equation 6 simplifies to

$$\Delta E_{ij} = 5.034 \times 10^{15} D[\cos\theta - 3\cos\phi\cos\phi']R_{ij}^{-3}\ \text{cm}^{-1} \qquad (7)$$

where 1 erg = 5.034×10^{15} cm^{-1} and D is the dipole strength, determined from the UV-visible spectrum of XBR to be approximately 44×10^{-36} cgs.[31] Substitution gives $\Delta E_{ij} \simeq +1000$ cm^{-1}, and since the value is positive, the α excited state is lower energy (longer wavelength) than the β state (Figure 8).

For a chiral molecular exciton, the two excited states (α and β) have been shown to give oppositely signed rotatory strengths, R^α and R^β:

$$R^{\alpha,\beta} = \pm(\pi/2)\sigma_0\cdot\vec{R}_{ij}\cdot(\vec{\mu}_{i0q} \times \vec{\mu}_{j0q}) \qquad (8)$$

where the upper and lower signs are associated with the α and β excited states, respectively, and σ_0 is the excitation energy of the pyrromethenone in cm^{-1}, taken here as 410 nm or 24 390 cm^{-1} for XBR. For a bilirubin with C_2 symmetry, the α state corresponds to B symmetry and the β state to A symmetry.[27] For the enantiomer (A, Figure 1) with left-handed helicity (of $\vec{\mu}_{i0q} \times \vec{\mu}_{j0q}$), the triple product $\vec{R}_{ij}\cdot(\vec{\mu}_{i0q} \times \vec{\mu}_{j0q}) < 0$ and therefore R^α takes a negative value and R^β takes a positive value. Since the α excited state is lower in energy than the β excited state, a (–) long-wavelength CE will be followed by a (+) shorter wavelength CE in the exciton couplet E^α,E^β. This corresponds to a negative exciton chirality, where exciton chirality may be defined as $\vec{R}_{ij}\cdot(\vec{\mu}_{i0q} \times \vec{\mu}_{j0q})(2\Delta E_{ij})$, as shown in Figure 8.

Thus, both here and in the general case[26] the handedness of screw sense that the electric dipole transition moments of the coupled pyrromethenone chromophores make with each other (Figures 4 and 8) correlates with signed order of the bisignate CD CEs. A left-handed screw sense (negative chirality) of the transition moments leads to a (–) longer wavelength CE followed by a (+) shorter wavelength CE. For a right-handed screw sense (positive chirality) the CE signs are inverted: (+) at the longer wavelength and (–) at the shorter wavelength component of the bisignate CE. Given the direction of the electric dipole transition moment in the pyrromethenone chromophore,[30] the exciton model can be used to predict the CE signs of the pigment in the structurally well-defined diastereomers, S·A and S·B (Figure 4), or the CE signs of the bilirubin enantiomers, A and B (Figure 1). In these intramolecularly hydrogen-bonded conformations, the relative orientations of the two pyrromethenone electric dipole moments constitute a left-handed chirality for S·A and A and a right-handed chirality for S·B and B. Accordingly, theory predicts a predominance of the left-handed diastereomeric complex S·A for solutions of BR-IX in the presence of quinine or cinchonidine since the induced bisignate CD shows a (–) CE near 465 nm followed by a (+) CE near 415 nm (Table I). By analogy, an excess of the right-handed diastereomeric complex S·B is favored in the presence of quinidine and cinchonine (Tables I–III). The predominant chirality of MBR-IV, BRDME, and MBRDME in the presence of quinine might also be deduced from the data of

(31) The UV spectrum of XBR was scanned in DMSO solvent in order to ensure measurements on monomers. (Pyrromethenones are known to dimerize in solution via amide-to-amide type intermolecular H bonds. See ref 16b and Falk et al. (Falk, H.; Grubmayr, K.; Höllbacher, G.; Hofer, O.; Leodolter, A.; Neufingerl, F.; Ribó, J. M. *Monatsh. Chem.* **1977**, *108*, 1113–1129). See also: Falk, H. In *Bile Pigments and Jaundice*; Ostrow, J. D., Ed.; Marcel Dekker: New York, 1986; Chapter 2.) The measured values were $\epsilon_{410} = 30\,000$ L·mol^{-1} cm^{-1}, $\Delta\sigma = 2250$ cm^{-1}, and $D = 44 \times 10^{-36}$ cgs.

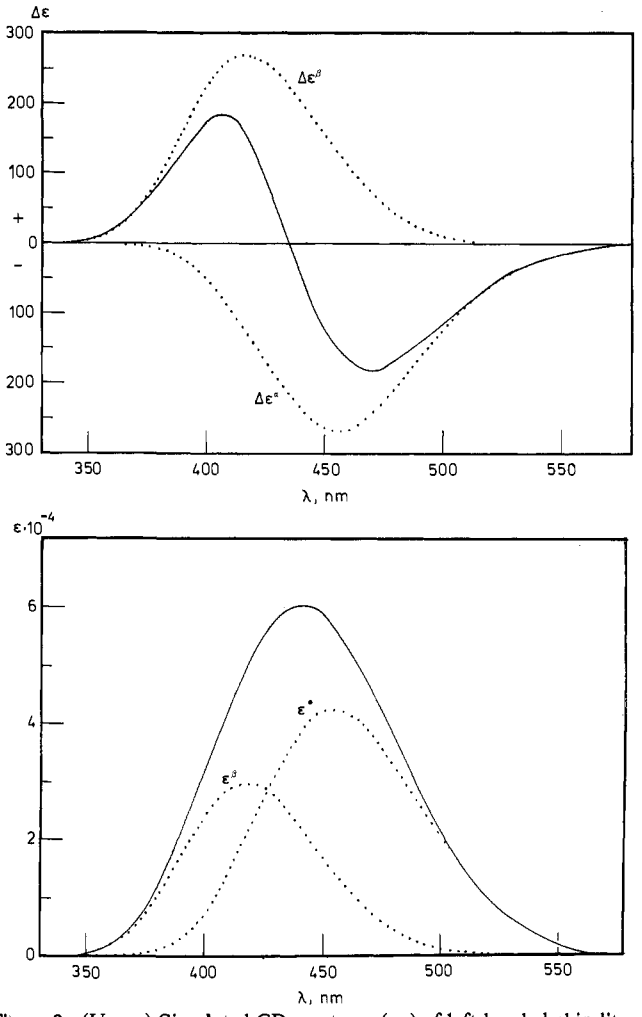

Figure 9. (Upper) Simulated CD spectrum (—) of left-handed-chirality bilirubin enantiomer (A) or diastereomeric complex (S·A). The two exciton bands (···) centered near 470 and 410 nm, corresponding to $0 \rightarrow E^{\alpha}$ and $0 \rightarrow E^{\beta}$, respectively, are represented by Gaussian shapes. The half-width $\Delta\sigma$ is assigned as 2300 cm^{-1}, and σ_0 is taken to be 23 000 cm^{-1}, $\Delta\epsilon^{\alpha}_{max} = -270$ L·mol^{-1}·cm^{-1}, $\Delta\epsilon^{\beta}_{max} = +270$ L·mol·cm^{-1}, and $\Delta E_{ij} \simeq 1000$ cm^{-1}. The dotted lines (···) show that the two calculated, overlapping, oppositely signed bands add together to give the simulated (—) exciton CD spectrum. (Lower) Simulated UV–visible spectrum (—) of A or S·A. The two Gaussian exciton bands (···) differ in intensity, with $\epsilon^{\alpha}_{max} = [(\tan\theta/2)]^2\epsilon^{\beta}$, where $\theta \simeq 100°$ and $\epsilon^{\beta}_{max} \simeq 30\,000$ L·mol^{-1}·cm^{-1}. The composite simulated UV–visible curve (—) shows the asymmetry characteristic of adding together two bands of unequal $\epsilon(\sigma)$.

Table V and exciton coupling theory. However, for these pigments we cannot at present point to well-defined conformations as we could with BR-IX.

Computed $\Delta\epsilon$ and Diastereomeric Excess of Bilirubin–Quinine Complex. The diastereomeric excess of the predominant chiral complex (S·A or S·B), and hence an exact measure of the equilibrium constant for, e.g., eq 3, is difficult to determine without quantitative CD or rotation data for the pure diastereomer. Thus, a large value for $\Delta\epsilon_{max}$, e.g., $\Delta\epsilon_{max} = 50$ L·mol^{-1}·cm^{-1}, might represent a large diastereomeric excess if the diastereomerically pure complex had $\Delta\epsilon_{max} = 100$ L·mol^{-1}·cm^{-1}, but only a relatively small diastereomeric excess if the pure diastereomer had $\Delta\epsilon_{max} = 1000$ L·mol^{-1}·cm^{-1}. Experimental CD or rotation values for diastereomerically pure complexes and the bilirubin enantiomers (A or B) are currently unavailable. They can, however, be calculated approximately by exciton coupling theory.[26] In our approach, we assumed that the conformation of the pigment in the complex S·A or S·B is not too different from that of enantiomers A and B, respectively. For further simplification, we focused our computations on a model in which two identical pyrromethenone chromophores (XBR) are held in chiral conformation of A. Since

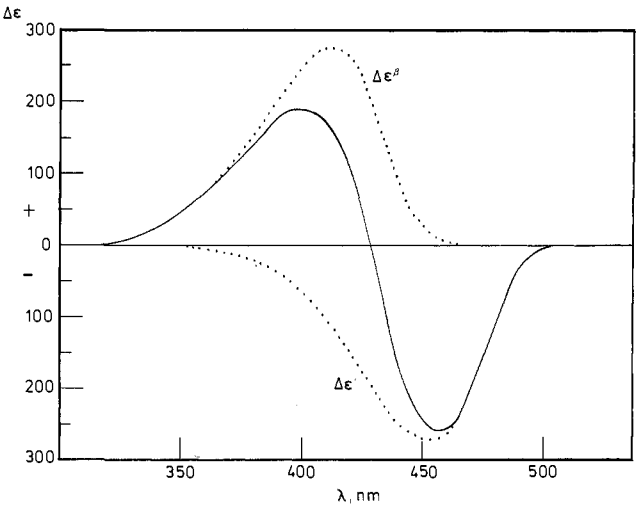

Figure 10. Simulated CD spectrum (—) of left-handed-chirality A or S·A obtained by adding together the two exciton component CD bands (···), with the band shapes corresponding to the experimentally observed UV–visible spectrum of XBR.[31] The $\Delta\epsilon^{\alpha}(\sigma)$ values are taken as $-270[(\epsilon(\sigma)/\Delta\epsilon_{max})$ for XBR] and $\Delta\epsilon^{\beta}(\sigma) = +270[(\epsilon(\sigma)/\Delta\epsilon_{max})$ for XBR] with the bands centered at $(\sigma_0 - \Delta E_{ij})$ and $(\sigma_0 + \Delta E_{ij})$ for the α and β excited states, respectively. $\sigma_0 \simeq 23\,000$ cm^{-1} and $\Delta E_{ij} \simeq 1000$ cm^{-1}.

our aim is to compute the magnitudes and signs of $\Delta\epsilon_{max}$ for the long-wavelength bisignate CD, we will need to determine and sum the $\Delta\epsilon(\sigma)$ values for each of the computed overlapping CD transitions of the exciton. As shown in the following, $\Delta\epsilon(\sigma)$ is related to the rotatory strengths of the CD transitions and to the energy separating them.

Our computations of R follow the examples of Harada and Nakanishi[26] and use the model shown in Figure 8 and eq 8 to give $R^{\alpha} \simeq -10 \times 10^{-38}$ cgs and $R^{\beta} \simeq +10 \times 10^{-38}$ cgs. From these rotatory strength values, one can compute $\Delta\epsilon_{max}$ and $\Delta\epsilon(\sigma)$ for the α and β states using the integrated form of the rotatory strength equation and assuming a Gaussian distribution for the CD CEs.

$$\Delta\epsilon^{\alpha,\beta}_{max} = (\sigma^{\alpha,\beta}/\Delta\sigma)(2.296 \times 10^{-39}\pi^{1/2})^{-1}R^{\alpha,\beta} \qquad (9)$$

where $\sigma^{\alpha,\beta}$ $(=\sigma_0 \pm \Delta E_{ij})$ is the wavenumber of the maximum value of $\Delta\epsilon$ $(\Delta\epsilon^{\alpha,\beta}_{max})$ and $\Delta\sigma$ is the bandwidth at $\Delta\epsilon_{max}/e$.[31] We take $\sigma^{\alpha,\beta}/\Delta\sigma \simeq \sigma_0/\Delta\sigma \simeq 10.9$ for the UV curve of XBR; therefore, $\Delta\epsilon^{\alpha}_{max} \simeq -270$ and $\Delta\epsilon^{\beta}_{max} \simeq +270$ L·mol^{-1}·cm^{-1}, and the $\Delta\epsilon_{max}$ are separated by the exciton splitting energy $2\Delta E_{ij}$.

Since the CD curves of the α and β excited states overlap, with some cancellation of intensity in the region between the band centers, the actual $\Delta\epsilon_{max}$ values "observed" will be smaller in magnitude and their λ_{max} will be shifted to longer and shorter wavelengths than their counterparts for $\Delta\epsilon^{\alpha}$ and $\Delta\epsilon^{\beta}$, respectively. They can be determined by summing $\Delta\epsilon^{\alpha}(\sigma)$ and $\Delta\epsilon^{\beta}(\sigma)$ over the wavelength range:

$$\Delta\epsilon^{\alpha,\beta}(\sigma) = (2.296 \times 10^{-39}\pi^{1/2})^{-1}(\sigma^{\alpha,\beta})(R^{\alpha,\beta})e^{-[(\sigma-\sigma^{\alpha,\beta})/\Delta\sigma]^2} \qquad (10)$$

A plot of $\Delta\epsilon^{\alpha}(\sigma) + \Delta\epsilon^{\beta}(\sigma)$ is shown in Figure 9. We chose to center the $0 \rightarrow q$ transition at ~23 000 cm^{-1}, the crossover point in the bilirubin–quinine CD spectra (Table II), and adopted a value of $\Delta\sigma \simeq 2300$ cm^{-1}.[32] The calculated UV–visible spectrum is also displayed in Figure 9. Here the two ϵ_{max} are not equal. Since the angle (θ) between $\vec{\mu}_{i0q}$ and $\vec{\mu}_{j0q}$ is approximately 100°, $\epsilon^{\alpha} = [\tan(100/2)]^2\epsilon^{\beta}$,[26] and the summed curve shows the characteristic asymmetry of bilirubin UV–visible spectra. Using Gaussian-shaped CD curves, one finds that the observed $\Delta\epsilon_{max}$ are equal (Figure 9). The experimental values are not equal, however, presumably due to Franck–Condon effects in electronic excitation, which makes the UV and CD bands steeper on the long-wavelength side.[26] With the assumption that the shapes of the indi-

(32) The UV–vis spectrum of mesobilirubin-XIIIα (the "molecular dimer" of XBR) shows $\epsilon_{431} \simeq 60\,000$ and $\Delta\sigma \simeq 2300$ cm^{-1} in $CHCl_3$.

vidual CD exciton bands correspond to that of the UV-visible spectrum of XBR,[31] the CD of A (Figure 1) or S·A (Figure 4) may be calculated and plotted as shown in Figure 10. Here the asymmetry in the curve shape is evident, and from the composite CD curve one finds $\Delta\epsilon_{max}^{455}$ −260 and $\Delta\epsilon_{max}^{395}$ +190 L·mol^{-1}·cm^{-1}. With these calculated values as references, the maximum experimental $\Delta\epsilon$ value (−135 L·mol^{-1}·cm^{-1} at 433 nm) for BR-IX + quinine in CH_2Cl_2 (Table II) corresponds to a ~50% diastereomeric excess of the complex corresponding to S·A (Figure 4).

Concluding Remarks

BR-IX and related rubins with propionic acid or propionate groups located at C-8 and C-12 tend to adopt either of two intramolecularly H-bonded enantiomeric conformations A and B (Figure 1) and as such may be viewed as racemic mixtures of interconverting mirror-image structures. Enantioselective binding to chiral solvating agents generates diastereomeric complexes, e.g., Figure 4, in which one diastereomer is favored over the other. As a consequence, BR-IX solutions become optically active in pigment and exhibit bisignate CD CEs, the intensity of which depends on the binding constant to the chiral solvating agent and its enantioselectivity. The very large bisignate CEs, previously characteristic only of albumin and other protein complexes with BR-IX,[7,8] can be detected for certain amines (cinchona alkaloids), which appear to bind to BR-IX with a high degree of enantioselectivity. We suggest that the binding enantioselectivity is high because of molecular complementarity at the dissymmetric microenvironment of the binding sites, e.g., amine salt formation stabilized by added H-bonding from a nearby secondary hydroxyl and π-π London force binding of the alkaloid quinoline aromatic system to a pigment pyrromethenone moiety. This type of chiral recognition, involving a similar sort of multiple-point binding, is probably responsible for the enantioselectivity implied by the intense bisignate ICDs of the bilirubin-albumin complex. Some of the same complementarity is potentially available at the albumin binding site, which is known to contain lysine as well as tryptophan groups.[12,13]

Conformations such as A and B (Figure 1) and S·A and S·B (Figure 4) appear to be essential in understanding the origin of the intense bisignate ICD CEs. Those bichromophoric pigments (MBR-IV, BRDME, and MBRDME) that cannot or do not adopt such conformations give only relatively weak, albeit bisignate, ICD CEs in the presence of cinchona alkaloids. Consequently, although we view all the bichromophoric pigments of this study as potential molecular excitons, only BR-IX shows bisignate ICD data characteristic of exciton systems wherein the two chromophores are held in the well-defined geometry (Figure 1 and 4) necessary for near-optimal orientation (skew angle of $\simeq$100°)[26] of their relevant electric dipole transition moments.

Acknowledgment. We thank the National Institutes of Health (Grant HD-17779) for generous support of this work. J.K.G. was on leave from Adam Mickiewicz University, Poznan, Poland (Program RP II.13.2.10), when this study was initiated.

Concertedness in Acyl Group Transfer in Solution: A Single Transition State in Acetyl Group Transfer between Phenolate Ion Nucleophiles

Salem Ba-Saif, Ajay K. Luthra, and Andrew Williams*

Contribution from the University Chemical Laboratory, Canterbury CT2 7NH, England. *Received February 11, 1987*

Abstract: Rate constants have been measured for nucleophilic substitution of 4-nitrophenol from 4-nitrophenyl acetate by a series of phenolate anions. The Brønsted type plot is linear for unhindered phenolate ions with pK_a values significantly above and below that of the displaced 4-nitrophenol: ($\log k_{ArO} = 0.75pK^{ArOH} - 7.28$; $n = 17$, $r = 0.984$); this is consistent with a mechanism involving a single transition state or a mechanism with an intermediate that has a very low barrier to decomposition. A small change in effective charge on the carbonyl group from reactant to transition state (measured from β_{nuc} and the known β_{eq} for the overall reaction) points to an almost coupled concerted mechanism for the transfer of the acetyl function between phenolate ion nucleophiles. The conclusions of this work are consistent with previous results that indicate relatively stable tetrahedral intermediates in reactions at reactive acyl centers; a spectrum of mechanisms exists for substitution reactions of acyl functions in solution that ranges from S_N1 (or ElcB for an ester with an α-carbanion) through concerted to BAc2.

Since the discovery of carbonyl oxygen exchange in the hydrolysis of alkyl esters[1] the solution chemistry of nucleophilic displacement at carbonyl functions has been dominated by the idea of tetrahedral intermediates.[2] The concept of a stable tetrahedral intermediate has been successfully challenged for those nucleophilic substitution reactions at acyl groups that possess good leaving functions and the potential to form an acylium ion intermediate (RCO^+) that may be stabilized by charge neutralization.[3a] These well-established mechanisms represent two extremes of timing of bond formation and fission for nucleophilic substitution. A third timing possibility could exist: namely, the process where nucleophile and leaving group form and break bonds simultaneously. The spectrum of mechanisms can be represented by the schematic free energy diagram (Figure 1). A coupled concerted mechanism[3b] where there is no imbalance between bond formation and fission involves a reaction coordinate along the north-east diagonal of this diagram; concerted pathways, involving no intermediates and a single transition state, can in principle traverse any area of the diagram not possessing an energy well.

A distinction between a concerted and an associative stepwise mechanism for a displacement reaction (for example, eq 1) can be achieved by a study of substituent effects on the nucleophile. The rate-limiting step for eq 1 will be k_1 for phenolate ions strongly basic compared with 4-nitrophenolate ion and k_2 for weakly basic

(1) Bender, M. L. *J. Am. Chem. Soc.* **1951**, *73*, 1626.
(2) (a) McClelland, R. A.; Santry, L. J. *Acc. Chem. Res.* **1983**, *16*, 394. (b) Capon, B.; Ghosh, A. K.; Grieve, D. M. A. *Ibid.* **1981**, *14*, 306.
(3) (a) Williams, A.; Douglas, K. T. *Chem. Rev.* **1975**, *75*, 627. (b) Jencks, W. P. *Chem. Soc. Rev.* **1981**, *10*, 345.

0002-7863/87/1509-6362$01.50/0